

available at [www.sciencedirect.com](http://www.sciencedirect.com)journal homepage: [www.elsevier.com/locate/biochempharm](http://www.elsevier.com/locate/biochempharm)

# Benzo[a]pyrene inhibits osteoclastogenesis by affecting RANKL-induced activation of NF- $\kappa$ B

I. Voronov<sup>a,b,\*</sup>, K. Li<sup>b</sup>, H.C. Tenenbaum<sup>a,b</sup>, M.F. Manolson<sup>b</sup>

<sup>a</sup> Department of Laboratory Medicine and Pathobiology, University of Toronto, Toronto, Canada

<sup>b</sup> Faculty of Dentistry, University of Toronto, Toronto, Canada

## ARTICLE INFO

### Article history:

Received 19 December 2007

Accepted 19 February 2008

### Keywords:

NF- $\kappa$ B

Osteoclasts

RANKL

Benzo[a]pyrene

AhR

## ABSTRACT

Exposure to polycyclic aryl hydrocarbons is linked to cancer, immunosuppression and other numerous health problems. We previously demonstrated that exposure to benzo[a]pyrene (BaP), an environmental pollutant present in high concentrations in urban smog and cigarette smoke, inhibits osteoclast differentiation and bone resorption. We hypothesized that this inhibition could be due to crosstalk between the receptor activator of NF- $\kappa$ B ligand (RANKL) and AhR signaling cascades competing for NF- $\kappa$ B, a common transcription factor for both pathways. RAW264.7 cells (a mouse macrophage cell line capable of differentiating into osteoclasts in the presence of RANKL) were exposed to different concentrations of RANKL and BaP and the effect on NF- $\kappa$ B activation, nuclear translocation, as well as the effect of NF- $\kappa$ B inhibitors on BaP-mediated CYP1B1 gene expression was measured. The results demonstrated that BaP inhibited both RANKL-induced NF- $\kappa$ B activation and nuclear translocation. At the same time, BaP-induced CYP1B1 gene expression was inhibited by two NF- $\kappa$ B inhibitors in a dose-dependent manner, demonstrating that NF- $\kappa$ B is involved in a BaP-mediated signaling pathway. A reporter gene assay showed that both BaP and RANKL-induced luciferase reporter gene transcription under the control of NF- $\kappa$ B response elements. Co-immunoprecipitation results demonstrated that AhR interacted with NF- $\kappa$ B p65 in RAW cells and BaP appeared to enhance this interaction. However, in the presence of RANKL, we did not observe any interaction between AhR and p65. These results support our hypothesis that BaP-mediated inhibition of osteoclastogenesis is a consequence of crosstalk between AhR and RANKL signaling pathways competing for the common transcription factor NF- $\kappa$ B.

© 2008 Elsevier Inc. All rights reserved.

## 1. Introduction

The deleterious effects of pollution on the environment and human health are becoming increasingly evident in today's

industrialized society. Polycyclic aryl hydrocarbons (PAHs) are ubiquitous environmental pollutants formed as a result of incomplete combustion of organic matter [1]. Common sources of PAHs include vehicle exhaust fumes from gasoline

\* Corresponding author at: Faculty of Dentistry, University of Toronto, 124 Edward Street, Room 400, Toronto, ON M5G 1G6, Canada. Tel.: +1 416 979 4900x4574; fax: +1 416 979 4936.

E-mail address: [irina.voronov@utoronto.ca](mailto:irina.voronov@utoronto.ca) (I. Voronov).

Abbreviations: AhR, aryl hydrocarbon receptor; ARNT, aryl hydrocarbon receptor nuclear translocator; BaP, benzo[a]pyrene; CYP1B1, cytochrome P450 1B1; DMSO, dimethyl sulfoxide; I $\kappa$ B $\alpha$ , inhibitor of nuclear factor  $\kappa$ B  $\alpha$ ; NF- $\kappa$ B, nuclear factor  $\kappa$ B; RANK, receptor activator of nuclear factor  $\kappa$ B; RANKL, receptor activator of nuclear factor  $\kappa$ B ligand; PAH, polycyclic aryl hydrocarbon.

0006-2952/\$ – see front matter © 2008 Elsevier Inc. All rights reserved.

doi:10.1016/j.bcp.2008.02.025

and diesel engines, smog [2], cigarette smoke and barbecued food [3]. Exposure to PAHs has been linked to cancer, immunosuppression, thymic atrophy, decreased resistance to viral and bacterial infections and diminished cytokine production [1]. PAHs induce many of their toxic effects via the aryl hydrocarbon receptor (AhR), a ligand-dependent transcription factor, resulting in enhanced expression of numerous genes, including phase I and phase II detoxification enzymes [4,5], such as cytochrome P450 1A1 (CYP1A1), CYP1B1 and CYP1A2. Of specific interest to us, AhR has been suggested to be involved in smoking-related impaired bone healing [6,7]. AhR belongs to the basic Helix-Loop-Helix/Per-ARNT-Sim (bHLH/PAS) motif family of proteins. Upon binding to PAHs, AhR translocates into the nucleus and dimerizes with AhR nuclear translocator (ARNT). The AhR/ARNT complex then binds to the aryl hydrocarbon receptor response elements (AHREs) to initiate gene transcription. It is known that AhR also interacts directly with coactivators/corepressors, as well as with other transcription factors, such as retinoblastoma protein (Rb) and NF- $\kappa$ B [8,9]. AhR is a ubiquitously expressed protein involved not only in detoxification of xenobiotics, but also in cell proliferation, differentiation and organogenesis [9].

Bone is a dynamic tissue that is constantly being remodeled. Two major cell types are responsible for this remodeling: osteoclasts, which resorb bone, and osteoblasts, which form bone. Osteoclasts are multinucleated cells formed by fusion of mononuclear precursors in the presence of receptor activator of nuclear factor  $\kappa$ B ligand (RANKL), a cytokine necessary for osteoclast differentiation, activation and survival [10]. The binding of RANKL to the RANK receptor on the surface of osteoclast progenitors [11] is followed by a signal transduction cascade and activation of transcription factors such as nuclear factor of activated T cells c1 (NFATc1), activator protein-1 (AP-1), and NF- $\kappa$ B [10].

The NF- $\kappa$ B family of proteins is known to regulate inflammatory response, apoptosis, tissue development, response to environmental stress, and it consists of five proteins: p65/RelA, c-Rel, RelB, NF- $\kappa$ B1 (p105/p50) and NF- $\kappa$ B2 (p100/p52). NF- $\kappa$ B1 and NF- $\kappa$ B2 proteins form homo- and heterodimers with the Rel proteins, with p65/p50 being the most common dimer. The dimers are located in the cytosol in an inactive state bound to the inhibitory I $\kappa$ B proteins (I $\kappa$ B $\alpha$ , I $\kappa$ B $\beta$ , and I $\kappa$ B $\epsilon$ ). NF- $\kappa$ B is considered to be one of the essential transcription factors for osteoclastogenesis since inhibition of this transcription factor or other proteins in the NF- $\kappa$ B signaling pathway results in absence or significant reduction of osteoclast formation [12].

We previously demonstrated that benzo[a]pyrene (BaP), a typical polycyclic aryl hydrocarbon present in cigarette smoke and smog at high concentrations [2,3,13,14], directly inhibited osteoclastogenesis and bone resorption [15]. Furthermore, this inhibition could be reversed by either the AhR antagonist resveratrol or high RANKL concentrations. Moreover, high concentrations of RANKL significantly decreased BaP-induced CYP1B1 gene expression, suggesting that there is crosstalk between the RANKL and AhR signaling pathways. Based on these results, we hypothesized that AhR and RANKL signaling pathways interact by competing for common transcription factors. Here, we investigate the role of NF- $\kappa$ B, a key transcription factor involved in osteoclast differentiation, in RANKL–AhR signaling crosstalk.

## 2. Materials and methods

### 2.1. Chemicals

BaP and DMSO were purchased from Sigma. Dulbecco's modified Eagle's medium (DMEM), fetal bovine serum, penicillin, streptomycin, TRIzol were purchased from Invitrogen. TransAM NF- $\kappa$ B p65 ELISA kit was purchased from ActiveMotif. NF- $\kappa$ B p65, I $\kappa$ B $\alpha$  antibodies, as well as secondary antibodies conjugated to horse radish peroxidase, were purchased from Santa Cruz; biotinylated secondary antibody and fluorescein-conjugated streptavidin were purchased from Vector Laboratories, ARNT antibody was purchased from Abcam. Gliotoxin, SC-514 and cyclosporin A were obtained from Calbiochem.

### 2.2. Osteoclast differentiation from the RAW 264.7 cell line

The mouse macrophage cell line RAW 264.7 was obtained from the American Type Culture Collection (ATCC). These cells, when cultured in the presence of RANKL, differentiate into osteoclasts [11]. The cells were maintained in DMEM containing 10% FBS, 100  $\mu$ g/ml penicillin and streptomycin. The media also contained 0–200 ng/ml recombinant glutathione S-transferase-soluble RANKL (GST-sRANKL), 0.1% DMSO (vehicle) and  $10^{-5}$ – $10^{-6}$  M BaP, depending on the experimental group. All cultures were incubated at 37 °C in humidified air containing 5% CO<sub>2</sub>.

### 2.3. Transcription factor activity assay

To measure NF- $\kappa$ B p65 activation, the cells were plated in 100 mm tissue culture dishes, grown to confluence, and incubated in the presence of DMSO,  $10^{-5}$ – $10^{-6}$  M BaP, 25 ng/ml RANKL or 200 ng/ml RANKL for 30–60 min. Nuclear extracts were prepared and analyzed for transcription factor activation using the Active Motif TransAM ELISA kit. Protein concentrations of the nuclear extracts were determined by BioRad reagent (BioRad) and 3  $\mu$ g of protein/well was used for the NF- $\kappa$ B p65 assays. The assays were performed according to manufacturer's instructions. Briefly, nuclear extracts were incubated in a 96-well plate coated with oligonucleotides containing the corresponding consensus sites for NF- $\kappa$ B. Then, the primary antibody was used to detect epitopes, which are only accessible when the transcription factors are activated and bound to the target DNA. An HRP-conjugated secondary antibody was used to detect the signal by spectrophotometry.

### 2.4. Immunofluorescence

To observe the effect of BaP on NF- $\kappa$ B p65 nuclear translocation, cells were plated in 8-well chamber slides, allowed to attach overnight, and then exposed to DMSO,  $10^{-5}$ – $10^{-6}$  M BaP, and 0–200 ng/ml RANKL for 30 min. The cells were then fixed with 100% methanol at –20 °C for 20 min, blocked in 1% normal goat serum in PBS for 1 h, incubated with mouse monoclonal anti-p65 overnight at 4 °C, followed by biotinylated secondary antibody for 2 h, and fluorescein-conjugated streptavidin for 1 h at room temperature. The nuclei were counterstained with DAPI. The slides were observed using a

Leica DM IRE2 microscope and images were obtained using OpenLab software (Improvision, version 4.0.2). To quantify nuclear translocation, 5 images/group were taken and the number of total cells and the number of cells with NF- $\kappa$ B translocation was counted. The results of three independent experiments were pooled and statistical significance was determined by Student's t-test.

## 2.5. RT-PCR

RAW 264.7 cells were plated in 60 mm tissue culture dishes at  $0.9 \times 10^6$  cells/dish, allowed to attach overnight, pre-treated with the inhibitor (gliotoxin, SC-514 or cyclosporine A) for 30 min, and then exposed to DMSO,  $10^{-5}$  M BaP and corresponding concentrations of the inhibitor for 20 h. Total RNA was extracted using TRIzol reagent by following the manufacturer's protocol. Total RNA (3  $\mu$ g) was treated with DNase I (Invitrogen) at 1 unit of DNase I/ $\mu$ g RNA according to the manufacturer's protocol and then reverse transcribed using Revert Aid H<sup>-</sup> First Strand Kit (MBI Fermentas). PCR reactions were performed in 50  $\mu$ l volumes using HotStarTaq polymerase (Qiagen). The initial activation was performed at 95 °C for 15 min, followed by 45 s at 94 °C for denaturation, 1 min at 60 °C for annealing, 1 min at 72 °C for extension, and 10 min at 72 °C for a final extension. The cycle number, the annealing temperatures, and the oligonucleotide sequences are summarized in Table 1. PCR products were separated on a 1.5% (v/v) agarose gel and visualized using GeneSnap software version 4.00.00 (SynGene, UK).

## 2.6. Transfections and luciferase reporter gene activity assay

For transfections, RAW264.7 cells were seeded in 12-well plates ( $8 \times 10^5$  cell/well) and the transfection with pNF- $\kappa$ B-Luc plasmid (Stratagene) was performed using LipofectAMINE 2000 (Invitrogen).  $\beta$ -galactosidase control plasmid was used for normalization of transfection efficiency. The pCIS-CK negative control plasmid and pFC-MEKK positive control plasmid (Stratagene) were used in every experiment. A time course preliminary experiment was performed and the levels of luciferase activity in the presence and absence of RANKL were measured at 2, 4, 6 and 24 h (data not shown). A significant RANKL-induced increase in luciferase activity was first detected at 6 h. Similar results were obtained both at 6 and 24 h time points. To determine the effect of BaP on RANKL-induced luciferase activity, the cells were incubated for 24 h and then treated with DMSO or  $10^{-5}$  M BaP in the presence of 0, 25 or 200 ng/ml RANKL. The cells were further incubated for 6 h (data not shown) or for 24 h and the luciferase activity was

determined using the Luciferase Assay Kit (Stratagene).  $\beta$ -Galactosidase activity levels were measured using a  $\beta$ -galactosidase Assay Kit (Stratagene).

## 2.7. Co-immunoprecipitation and Western blotting

RAW264.7 cells were plated in 100 mm tissue culture dishes, grown to confluence and then treated at 37 °C with DMSO or  $10^{-5}$  M BaP in the presence or absence of 200 ng/ml RANKL for indicated time periods. At the end of the incubation period, the cells were washed twice with PBS, scraped in PBS and then lysed in 500  $\mu$ l of lysis buffer (50 mM Tris, pH 7.4, 300 mM NaCl, 1% Triton X-100, 5 mM EDTA, protease inhibitor cocktail (Sigma, P8340), phosphatase inhibitor cocktail (Sigma, P5726), and PMSF) for 20 min, centrifuged for 15 min at  $12,000 \times g$ , and the supernatant fraction was collected. A 40  $\mu$ l aliquot was removed from each sample for later use and the rest of the sample was used for IP. The whole cell lysates were incubated overnight with 5  $\mu$ g of anti-p65 NF- $\kappa$ B, ARNT antibody or IgG control (Santa Cruz) at 4 °C on a rotary shaker. Protein G sepharose (Amersham) slurry resuspended in lysis buffer was added to the samples and incubated for additional 2 h at 4 °C on a rotary shaker. The beads were washed three times with PBS and boiled in  $2 \times$  SDS sample buffer. Proteins were separated on 8% mini SDS-PAGE gel, transferred to a nitrocellulose membrane (Amersham Hybond-ECL) using a full immersion transfer apparatus (Bio-Rad) on ice at 75 V, 150 mAmps for 1 h, blocked with 5% milk in TBS-T buffer and then incubated with anti-AhR primary antibody (Biomol), anti-ARNT antibody, anti-I $\kappa$ B $\alpha$  or anti-NF- $\kappa$ B p65 antibody. The blots were incubated with 1:2000 dilution of a secondary HRP-conjugated antibody for 1 h at room temperature, washed and developed using ECL reagents (Perkin-Elmer Life Sciences). Images were captured using GeneSnap software version 4.00.00 (SynGene, UK).

## 3. Results

### 3.1. BaP inhibits RANKL-induced NF- $\kappa$ B nuclear translocation and activation

Exposure to cigarette smoke impairs bone healing [6,7]. As osteoclast activity is essential to bone healing, we asked if osteoclasts function was similarly affected. We previously demonstrated that BaP, a typical aryl hydrocarbon present in cigarette smoke, inhibits osteoclast formation and resorptive activity [15]. Here, we investigate the molecular mechanisms underlying the BaP-induced inhibition of osteoclasts focusing primarily on early signaling events using the same model of

**Table 1 – List of primers for RT-PCR**

Name	Forward (5' to 3')	Reverse (5' to 3')	T <sub>a</sub> (°C)	Cycles
GAPDH	TGCCAGCCTCGTCCCGTAGAC	CCTCACCCCATTTGATGTTAG	60	25
CYP1B1	GGCGTTCGGTCACTACTCTG	AGGTTGGGCTGGTCACTCAT	60	35
NFATc1	CAACGCCCTGACCACCGATAG	GGCTGCCTTCCGTCTCATAGT	60	25
c-Myc	CACCAGCAGCGACTCTGAAGAAGAG	AGAGGTGAGCTTGTGCTCGTCTGC	60	25

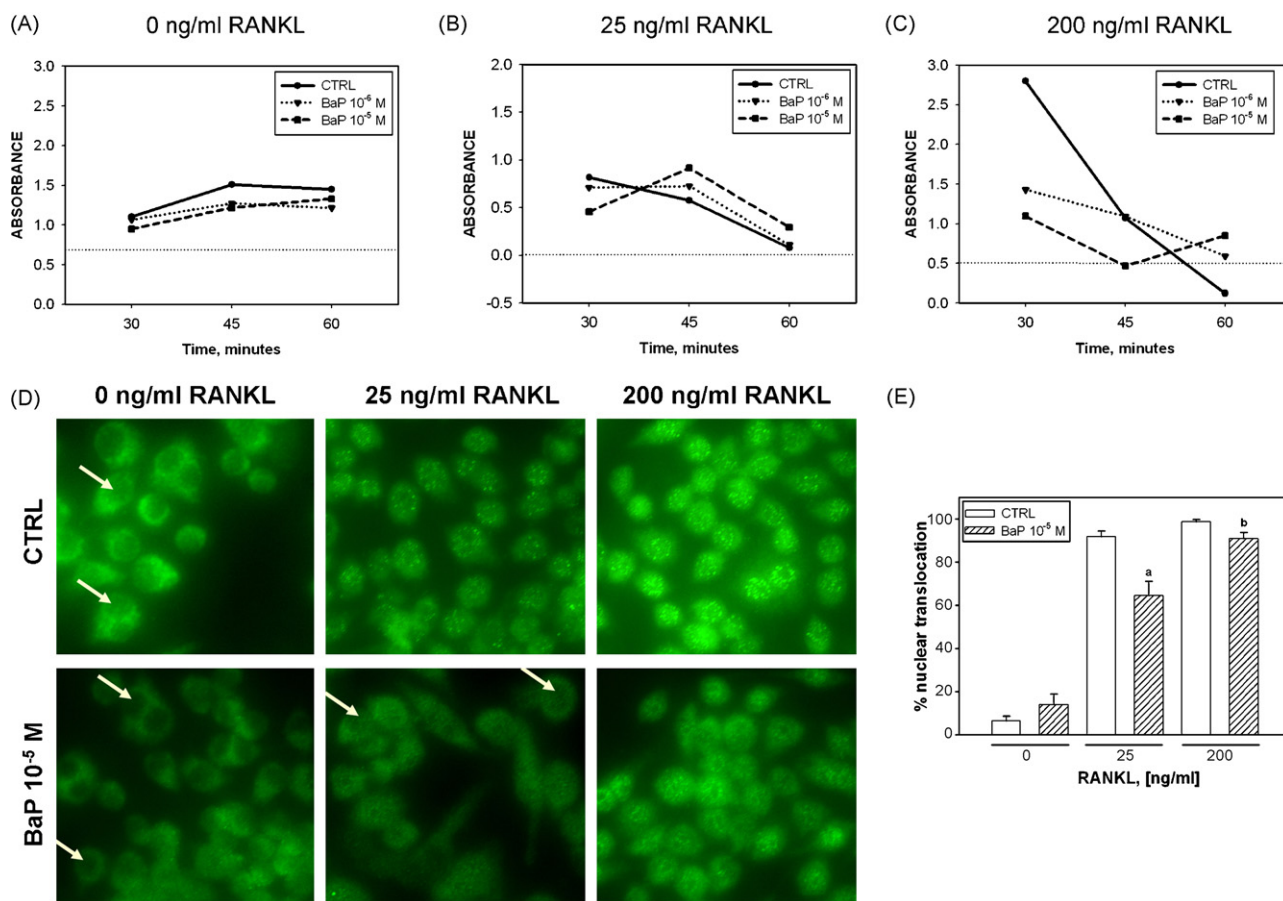


**Fig. 1 – BaP inhibits NF- $\kappa$ B activation at 25 and 200 ng/ml RANKL.** RAW264.7 cells were grown to confluence and then exposed to different concentrations of RANKL ((A) 0; (B) 25; (C) 200 ng/ml RANKL) and BaP for 30, 45 and 60 min. Nuclear extracts were analyzed for NF- $\kappa$ B activation using TransAM ELISA kit (Active Motif). The horizontal dotted line represents the level of NF- $\kappa$ B activation in unstimulated cells (no treatment). Similar results were obtained in two additional independent experiments. (D)  $10^{-5}$  M BaP decreases NF- $\kappa$ B nuclear translocation in RAW cells. The cells were treated with 0–200 ng/ml RANKL in the presence or absence of  $10^{-5}$  M BaP for 30 min, fixed, permeabilized, and incubated with anti-p65 (Santa Cruz). White arrows point out nuclei without NF- $\kappa$ B nuclear translocation; (E) quantification of NF- $\kappa$ B nuclear translocation. Cells were treated and stained as described above in (D). The total number of cells, as well as the number of cells showing nuclear translocation in five random fields per group was counted. The numbers for each experiment were pooled and the percent of cells showing nuclear translocation was calculated. CTRL indicates DMSO treated cells. The results are expressed as mean  $\pm$  S.D.,  $n = 3$ . (a, b) statistically different from corresponding controls,  $p < 0.05$ . Statistical analysis was performed using Student's  $t$ -test.

osteoclastogenesis: the RAW264.7 mouse macrophage cell line. These cells, when cultured in the presence of RANKL, differentiate into osteoclasts [11]. Since NF- $\kappa$ B is a key transcription factor activated by RANKL at early stages of osteoclastogenesis, we decided to first investigate the effect of BaP on RANKL-induced NF- $\kappa$ B activation.

NF- $\kappa$ B is a dynamic transcription factor and its nuclear translocation kinetics depend on the inducing agent [16]. It has been demonstrated that RANKL and tumor necrosis factor  $\alpha$  (TNF- $\alpha$ ) [17–19] induce a transient NF- $\kappa$ B response that peaks at around 30 min and is terminated by 60 min. To determine whether BaP affects RANKL-induced NF- $\kappa$ B activation, the cells were incubated with RANKL and BaP for 30, 45 and 60 min and the levels of activated NF- $\kappa$ B in the nuclear extracts were measured using TransAM kit (Fig. 1A–C). In the absence of

RANKL, DMSO causes a small and sustained increase in NF- $\kappa$ B activation as compared to unstimulated cells (indicated by the horizontal dotted line), and the addition of BaP did not alter this pattern. In the presence of 25 ng/ml RANKL for 30 min,  $10^{-5}$  M BaP in three independent experiments, consistently decreased RANKL-mediated activation of NF- $\kappa$ B, while  $10^{-6}$  M BaP had little or no effect compared to vehicle control. At 45 min, in 2 out of 3 experiments we observed an increase of NF- $\kappa$ B activity in the presence of  $10^{-5}$  M BaP compared to vehicle control. This increase could be due to a BaP-mediated shift of NF- $\kappa$ B activation in response to RANKL. By 60 min, RANKL-mediated NF- $\kappa$ B activation consistently decreased, while the presence of  $10^{-5}$  M BaP kept NF- $\kappa$ B levels elevated. Similar results were obtained at 200 ng/ml RANKL at the 30 min time point. However, at 45 min,  $10^{-5}$  M BaP still



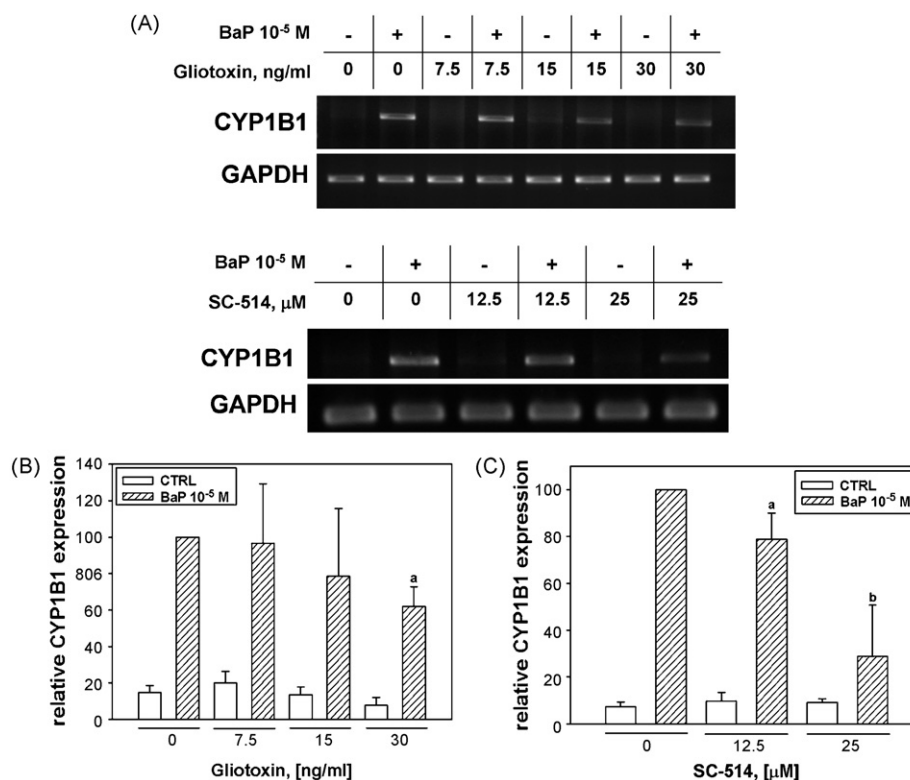


**Fig. 2** – NF- $\kappa$ B inhibitors, gliotoxin and SC-514, inhibit BaP-induced CYP1B1 mRNA expression in a dose-dependent manner. RAW cells were cultured for 24 h, pre-treated with the inhibitor for 30 min and then incubated in the presence of the inhibitor, 10<sup>-5</sup> M BaP, or DMSO for 20 h followed by RNA extraction. These samples were analyzed by RT-PCR and representative gels are shown in (A). The density of these bands was analyzed by GeneTools software. The values for CYP1B1 were normalized to the GAPDH value for each sample. The densitometry results shown in (B) and (C) are expressed as mean  $\pm$  S.D.,  $n = 3$ . (a, b) statistically different from a corresponding control (BaP 10<sup>-5</sup> M, no inhibitor),  $p < 0.05$ . Statistical analysis was performed using Student's  $t$ -test.

inhibited RANKL-induced activation in cells treated with 200 ng/ml of RANKL. By 60 min, NF- $\kappa$ B activation in BaP-containing groups was above the vehicle control levels. These results demonstrate that the presence of BaP inhibits RANKL-induced NF- $\kappa$ B activation at 30 min time point.

We then asked whether there is also an inhibitory effect of BaP on NF- $\kappa$ B nuclear translocation. Using immunofluorescence, BaP-mediated inhibition of NF- $\kappa$ B nuclear translocation was clearly visible at 25 ng/ml RANKL after 30 min of incubation (Fig. 1D). Quantification of the immunofluorescence confirmed these observations (Fig. 1E). This suggests that BaP affects not only NF- $\kappa$ B binding to DNA (TransAM activity assay) but also inhibits nuclear translocation of NF- $\kappa$ B.

### 3.2. NF- $\kappa$ B is necessary for BaP-mediated CYP1B1 expression

We previously demonstrated that RANKL inhibited BaP-induced CYP1B1 gene expression suggesting that both BaP and RANKL use the same transcription factor for signal transduction [15]. To investigate the involvement of NF- $\kappa$ B in BaP-induced CYP1B1 expression, the cells were incubated in the presence of gliotoxin or SC-514 and the levels of CYP1B1 mRNA were determined by RT-PCR. Gliotoxin and SC-514 are

commonly used inhibitors of NF- $\kappa$ B but they have different mechanisms of action. At high concentrations, gliotoxin prevents NF- $\kappa$ B-DNA binding, whereas at low concentrations it prevents I $\kappa$ B $\alpha$  degradation [20–22]. SC-514 is a highly selective inhibitor of I $\kappa$ B kinase  $\beta$  (IKK $\beta$  or IKK2) shown to specifically block NF- $\kappa$ B dependent gene expression [23]. For these experiments, we used the highest inhibitor concentrations that did not affect cell viability (data not shown). RT-PCR results demonstrate that BaP-induced CYP1B1 mRNA levels significantly decreased with increasing concentrations of both inhibitors (gliotoxin and SC-514) in a dose-dependent manner (Fig. 2), while GAPDH gene expression was not affected. These results suggest that NF- $\kappa$ B is involved in BaP-induced CYP1B1 expression. Inhibition of this induction with the IKK $\beta$  specific inhibitor, SC-514, indicates the involvement of the canonical pathway [12].

### 3.3. NFATc1 is not involved in induction of CYP1B1 by BaP

We next asked whether NFATc1, another key transcription factor involved in osteoclastogenesis, is implicated in AhR-RANKL signaling crosstalk. NFATc1 belongs to the NFAT family of transcription factors that are evolutionary related to the NF- $\kappa$ B family. These proteins are regulated by Ca<sup>2+</sup> and

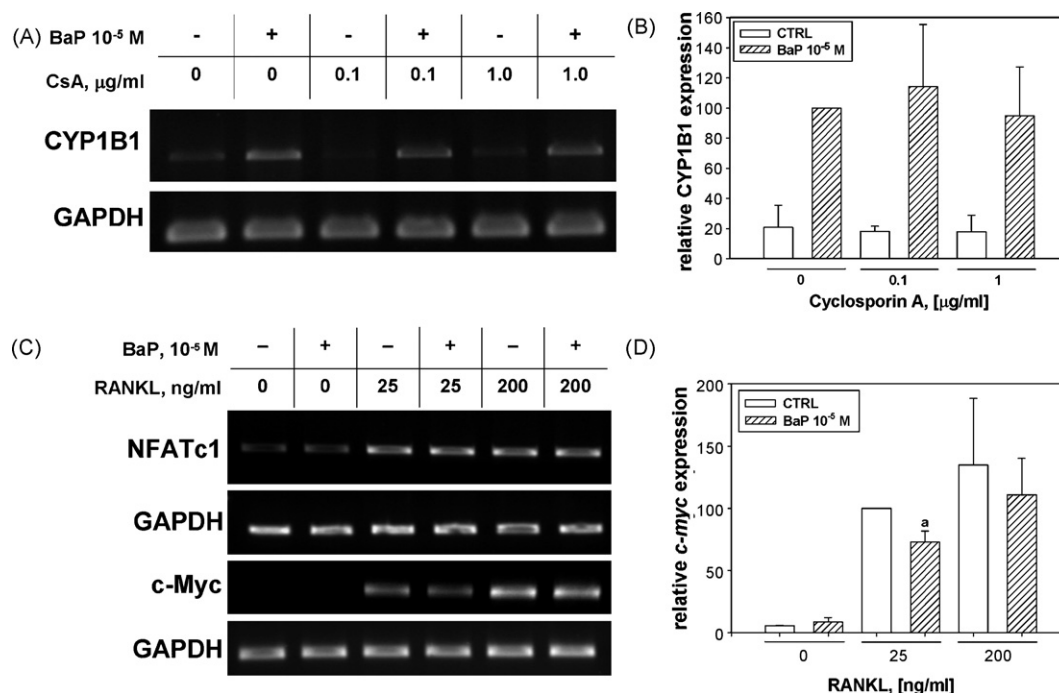


**Fig. 3 – The effect of BaP on CYP1B1, NFATc1, and c-Myc expression.** (A and B) RAW cells were cultured for 24 h, pre-treated with cyclosporin A (the inhibitor of NFATc1) for 30 min and then incubated in the presence of the same concentration of the inhibitor, 10<sup>-5</sup> M BaP, or DMSO for 20 h followed by RNA extraction. These samples were analyzed by RT-PCR and a representative gel is shown in (A). The density of the bands was analyzed by GeneTools software, the values for CYP1B1 were normalized to the GAPDH value for each sample. The densitometry results (B) are expressed as mean  $\pm$  S.D.,  $n = 3$ . (C) 10<sup>-5</sup> M BaP inhibits RANKL-induced c-myc gene expression in RAW cells, but has no effect on NFATc1 gene expression as determined by RT-PCR. The cells were cultured for 24 h and then treated with 0–200 ng/ml RANKL and 10<sup>-5</sup> M BaP or DMSO for 20 h followed by RNA extraction. Samples were analyzed by RT-PCR and a representative gels are shown in (C). Similar results were obtained in two additional experiments. (D) Quantification of c-myc expression. The values for c-Myc were normalized to the GAPDH value for each sample and expressed as a percent of vehicle control in the presence of 25 ng/ml RANKL. The densitometry results shown in (D) are expressed as mean  $\pm$  S.D.,  $n = 3$ . (a) Statistically different from a corresponding control,  $p < 0.05$ . Statistical analysis was performed using Student's t-test.

Ca<sup>2+</sup>/calmodulin-dependent serine phosphatase calcineurin [24]. To assess whether NFATc1 is involved in induction of CYP1B1 gene expression by BaP, the cells were treated with cyclosporin A, an inhibitor of the protein phosphatase activity of calcineurin. Exposure of RAW cells to cyclosporin A had no effect on induction of CYP1B1 mRNA by BaP as determined by RT-PCR (Fig. 3A and B). Furthermore, the RANKL-induced increase of NFATc1 gene expression was not affected by BaP treatment (Fig. 3C). These results indicate that NFATc1 is not involved in the AhR–RANKL signaling crosstalk.

### 3.4. BaP inhibits RANKL-induced c-Myc gene expression

We next asked whether BaP has an effect on RANKL-induced gene expression. c-Myc is one of the transcription factors involved in osteoclastogenesis and its transcription is regulated by NF- $\kappa$ B [25]. It has been demonstrated that c-Myc is expressed at very low levels in RAW cells, however, exposure to RANKL dramatically induces c-myc gene expression [26]. To see whether BaP has an effect on c-myc gene expression, the cells were analyzed by RT-PCR (Fig. 3C and D). The results demonstrate that in the presence of 25 ng/ml RANKL but not

200 ng/ml RANKL, BaP partially but significantly inhibited c-myc expression by about 30%. These results indicate that BaP inhibits RANKL-induced gene expression mediated by NF- $\kappa$ B.

### 3.5. BaP induces luciferase reporter gene transcription under the control of NF- $\kappa$ B response elements

To determine whether NF- $\kappa$ B is involved in mediating responses to BaP, RAW cells were transiently transfected with a plasmid containing 6 NF- $\kappa$ B response elements upstream of a luciferase reporter gene. As expected, 25 and 200 ng/ml RANKL increased luciferase activity (Fig. 4). Furthermore, BaP significantly increased the luciferase response on its own and showed an additive effect with the 25 and 200 ng/ml concentrations of RANKL after 6 h (data not shown) and also after 24 h of incubation (Fig. 4). These results further suggest that NF- $\kappa$ B is activated by both RANKL and BaP in a cumulative manner. These results are not inconsistent with NF- $\kappa$ B nuclear translocation and DNA binding assays shown in Fig. 1. Taken together, the data imply that BaP inhibits RANKL-induced NF- $\kappa$ B nuclear translocation and DNA binding at an early time point (30 min) but activates NF- $\kappa$ B at later time points (6–24 h).

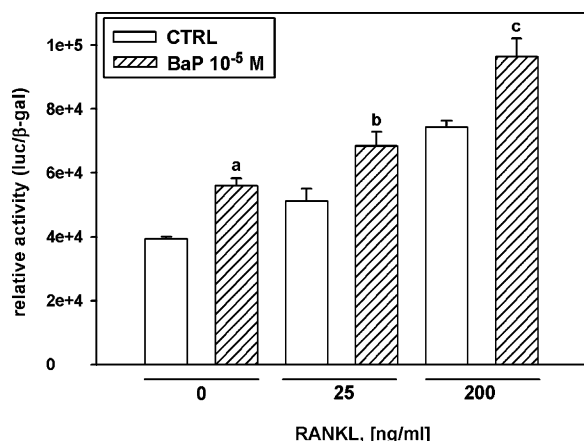


**Fig. 4 – RANKL and BaP induce luciferase reporter gene transcription under the control of NF- $\kappa$ B response elements.** RAW264.7 cells were transiently transfected with pNF- $\kappa$ B-Luc and  $\beta$ -gal plasmids and then incubated in the presence of  $10^{-5}$  M BaP, or vehicle control (DMSO) and 0–200 ng/ml RANKL for 24 h. To account for differences in transfection rates, the data were normalized to the constitutively expressed  $\beta$ -gal. The results are expressed as mean  $\pm$  S.D.,  $n = 3$ . (a, b, c) statistically different from corresponding controls,  $p < 0.05$ . Statistical analysis was performed using Student's t-test. Similar results were obtained in two additional independent experiments.

### 3.6. BaP enhances AhR/NF- $\kappa$ B interaction only in the absence of RANKL

As shown so far, NF- $\kappa$ B appears to be involved in both BaP and RANKL-mediated signaling pathways. Because AhR and NF- $\kappa$ B interact in both hepatoma and dendritic cells in the presence of dioxin [27,28], we used co-immunoprecipitation to ask if a similar interaction occurs in RAW cells. Interestingly, an anti-p65 antibody co-precipitated AhR and NF- $\kappa$ B in the absence but not in the presence of RANKL. Furthermore, in the absence of RANKL,  $10^{-5}$  M BaP increased the p65/AhR interaction at both 20 and 30 min (Fig. 5A and B). At the same time, interaction between AhR and ARNT was observed only in the presence of BaP and this interaction was not disrupted by 200 ng/ml RANKL (Fig. 5C). However, when the blots were probed with anti-p65 antibody, p65 was not detected in the AhR/ARNT complex (data not shown).

The absence or presence of BaP did not appear to substantially affect the amount of I $\kappa$ B $\alpha$  being pulled down by anti-p65. Furthermore, immunoblots of the whole cell lysates showed that BaP did not affect cellular I $\kappa$ B $\alpha$  levels at these time points (unpublished observations), confirming similar results by Ruby et al. [28]. In contrast, the interaction between I $\kappa$ B $\alpha$  and p65 decreased after 20 min exposure to 200 ng/ml RANKL and was restored by 120 min. These results are compatible with current literature showing that in the RANKL-mediated activation of the NF- $\kappa$ B pathway, I $\kappa$ B $\alpha$  is degraded after 10–20 min with protein levels restored in  $\sim$ 60 min [29].

These results demonstrate that in RAW264.7 mouse macrophage cell line AhR is present in a complex with NF-

$\kappa$ B and I $\kappa$ B $\alpha$  and that this interaction is disrupted upon NF- $\kappa$ B activation by RANKL.

## 4. Discussion

Here, we show for the first time that NF- $\kappa$ B is a transcription factor involved in both BaP- and RANKL-mediated signaling pathways in a mouse macrophage cell line. Furthermore, we present the novel finding that in a mouse macrophage cell line, NF- $\kappa$ B is involved in BaP-induced CYP1B1 gene expression.

The purpose of this project was to investigate the molecular mechanism by which BaP inhibits osteoclastogenesis. Osteoclasts are multinucleated cells formed by fusion of mononuclear precursor cells in the presence of RANKL. RANKL is a member of the TNF superfamily and it activates a number of transcription factors upon binding to its receptor RANK. As the name RANKL (Receptor Activator of NF- $\kappa$ B Ligand) implies, NF- $\kappa$ B is one of the major transcription factors activated by RANKL. At the same time, aryl hydrocarbons activate NF- $\kappa$ B via the AhR-mediated signaling pathway and this activation has been investigated by several groups. Increased DNA binding activity of NF- $\kappa$ B was observed in mouse hepatoma cells [30] and in human hepatoblastoma cells [31]. Direct NF- $\kappa$ B activation by BaP in a human epithelial cell line was confirmed using luciferase reporter gene assays [32]. NF- $\kappa$ B p50 and p65 nuclear translocation in thymic stromal cells induced by TCDD treatment was demonstrated *in vivo* and *in vitro* [33].

Therefore, this investigation of inhibition of osteoclastogenesis evolved into an investigation of two molecules that independently activate NF- $\kappa$ B. As mentioned before, NF- $\kappa$ B activation is a dynamic process, involving rapid degradation of I $\kappa$ Bs, translocation of NF- $\kappa$ B into the nucleus, re-synthesis of I $\kappa$ Bs and export of NF- $\kappa$ B out of the nucleus. The oscillations depend on the activating agent. RANKL induces a rapid but short-lived activation of NF- $\kappa$ B with the peak of activation around 30 min. Based on the available literature, it appears that BaP activation of NF- $\kappa$ B is of smaller amplitude. However, in contrast to RANKL, BaP causes a sustained activation of this transcription factor.

Since both BaP and RANKL activate NF- $\kappa$ B, one would expect a cumulative increase in the activation of this transcription factor as was seen in the luciferase reporter gene experiments (Fig. 4). In contrast, we observed that BaP inhibited RANKL-induced NF- $\kappa$ B nuclear translocation and DNA binding (Fig. 1). These results are not contradictory but rather suggest that BaP inhibits RANKL-induced NF- $\kappa$ B nuclear translocation and DNA binding at an early time point (30 min) and activates NF- $\kappa$ B at later time points (6–24 h). The results confirm published reports that PAHs activate NF- $\kappa$ B at later time points (2 h and up to 72 h) [30,32]. Moreover, NF- $\kappa$ B involvement in the BaP-mediated signaling pathway was confirmed by incubation with two different NF- $\kappa$ B inhibitors, resulting in a dose-dependent decrease of BaP-induced CYP1B1 gene expression.

The reciprocal inhibition between NF- $\kappa$ B activating agents and aryl hydrocarbons has been described before. Cytokines, such as TNF- $\alpha$  [27,34,35], interleukin-1 $\beta$  [36], interleukin-6 [36], and lipopolysaccharides [34,35] decrease cytochrome P450 enzyme expression and activity levels, possibly as a part of the

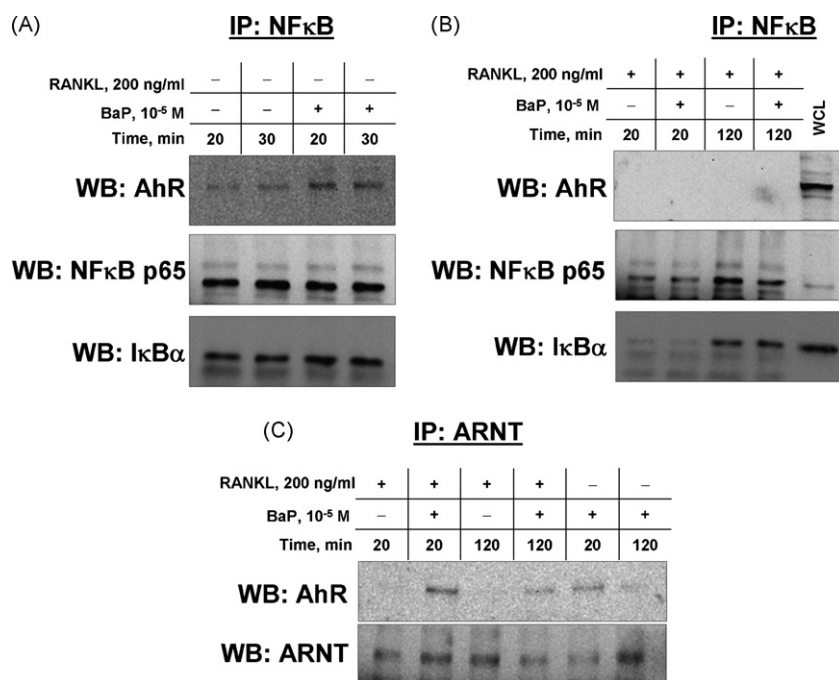


**Fig. 5 – BaP enhances AhR/NF-κB interaction only in the absence of RANKL:** RAW264.7 cells were grown to confluence and treated with DMSO or 10<sup>-5</sup> M BaP and/or 200 ng/ml RANKL for the indicated time periods. Whole cell lysates, obtained as described in Section 2, were incubated with anti-p65 (A and B) or anti-ARNT (C) antibodies and precipitated with protein G sepharose. Proteins were separated by SDS-PAGE, transferred to a nitrocellulose membrane and then incubated with anti-AhR, anti-ARNT, anti-IκBα and anti-p65 antibody. The blots were then incubated with HRP-conjugated antibody and resulting images were captured using GeneSnap (Syngene). WCL – whole cell lysate.

host-defense response mechanisms [37]. Moreover, it has been demonstrated that AhR and NF-κB physically interact and functionally modulate each other's activities in rat hepatoma cells [8,27]. Therefore, it has been proposed that there is crosstalk between AhR and NF-κB signaling pathways [8]. Our results confirm this hypothesis. Using co-immunoprecipitation, we demonstrated that AhR and p65 interact in RAW cells. This interaction was increased in the presence of BaP but was disrupted in the presence of RANKL. The co-immunoprecipitation of AhR and p65 in RAW cells corroborates the observation of AhR/p65 interaction in dendritic cells [28]. However, in contrast to our observation that RANKL disrupted this interaction, Ruby et al. [28] reported an enhancement of AhR/p65 interaction by TNF-α. This discrepancy could be explained by differences in cell type, incubation time points and the use of endogenous versus exogenous AhR (dendritic cells were transfected with AhR-FLAG in the experiments by Ruby et al.). Co-immunoprecipitation also revealed that RANKL-induced IκBα degradation was not affected by BaP, confirming the previous report that IκBα proteolysis was not affected by TCDD treatment [28]. RANKL treatment did not disrupt BaP-induced AhR/ARNT interaction at 20 and 120 min.

Our findings demonstrate that NF-κB is involved in the BaP-induced signaling pathway; however, the mechanism of NF-κB activation by BaP is still not known. This is not surprising considering that NF-κB activation is very complicated and tightly regulated; it is also stimulus- and cell type-specific, resulting in activation of either the canonical or alternative

pathways. In the following paragraphs we will speculate on a possible mechanism of NF-κB involvement in AhR-RANKL crosstalk. To do this we will first discuss separately the RANKL and AhR signaling pathways.

The mechanism of RANKL-mediated NF-κB activation is well understood [38,39]. Upon RANKL binding to RANK, several signaling proteins are recruited to the receptor, including TNF-α receptor associated factors (TRAFs) 2, 3, 5 and 6. TRAF6, a factor essential for osteoclastogenesis [39], is a RING domain E3 ubiquitin ligase that catalyzes synthesis of Lys-63 linked polyubiquitin chain [40,41]. This polyubiquitination activates the transforming growth factor β activated kinase-1 (TAK1) complex, which in turn phosphorylates IKKβ, leading to activation of the IKK complex. The IKK complex, which consists of IKKα, IKKβ and IKKγ, phosphorylates IκBα, therefore, targeting it for degradation. This allows NF-κB to translocate to the nucleus, bind to DNA and initiate gene expression.

The mechanism of BaP-induced NF-κB activation is not known. One possible scenario is that, analogous to TRAF6, AhR acts as a ligand-dependent E3 ubiquitin ligase [42], activates the IKK complex and consequently initiates the NF-κB signaling cascade. However, unlike RANKL, BaP-induced NF-κB activation would have much slower kinetics, resulting in NF-κB activation hours after the induction, rather than minutes.

Another open question is how AhR interacts with the NF-κB complex. Our results demonstrate that, in the absence of RANKL, AhR is present in a complex with NF-κB and IκBα.



However, the co-immunoprecipitation results cannot differentiate whether AhR interacts directly with NF- $\kappa$ B or with another protein in the complex. One possibility is a direct interaction between AhR and I $\kappa$ B $\alpha$ . Wu et al. demonstrated a direct Per-Arnt-Sim (PAS)-domain-dependent interaction between phosphodiesterase (PDE) 8A1, a PAS domain containing protein, and all I $\kappa$ B proteins as well as c-Rel and RelB, but not p65, p50 or p52 [43]. Based on their deletion studies, the authors hypothesized that the proteins interacted via the PAS domain of the PDE8A1 and the ankyrin-repeat motifs of I $\kappa$ Bs. The results of Wu et al. suggest that a similar interaction may exist between the PAS domain of AhR and the ankyrin-repeat motif of I $\kappa$ B $\alpha$  in mouse macrophages and osteoclast precursors.

Here, we propose the following mechanism of AhR–NF- $\kappa$ B crosstalk. In the absence of RANKL, a certain amount of AhR is present in the cytoplasm in a complex with p65 and I $\kappa$ B $\alpha$ . As suggested above, upon stimulation with BaP, AhR acts as a ligand-dependent E3 ubiquitin ligase and activates the IKK complex, resulting in NF- $\kappa$ B activation. The rest of AhR forms a complex with ARNT and binds to DNA as previously described [9]. Even though the exact mechanism of NF- $\kappa$ B participation in BaP-induced gene expression is not clear, our data show that it is necessary for CYP1B1 gene expression. It is possible that NF- $\kappa$ B is not directly involved in CYP1B1 gene expression, since the promoter region of mouse CYP1B1 does not contain known  $\kappa$ B elements [44,45]. In the presence of high concentrations of RANKL, due to fast activation kinetics, the IKK complex is activated within minutes of the induction, leading to rapid I $\kappa$ B $\alpha$  degradation and sequestering of NF- $\kappa$ B to RANKL-specific  $\kappa$ B elements. We speculate that the loss of I $\kappa$ B $\alpha$  breaks AhR interaction with NF- $\kappa$ B, and, as a result, making NF- $\kappa$ B no longer available for BaP-induced CYP1B1 expression and resulting either in inhibition or a delay of gene expression. In the presence of low concentrations of RANKL, both pathways are active. Since not all of I $\kappa$ B $\alpha$  is degraded, BaP-induced CYP1B1 expression is marginally inhibited by RANKL [15]. At the same time, RANKL-induced *c-myc* gene expression is also affected (Fig. 3) resulting in inhibition of osteoclastogenesis. Work is in progress in this laboratory to further test this proposed mechanism of AhR–NF- $\kappa$ B crosstalk.

In summary, here we present data that AhR–NF- $\kappa$ B crosstalk is a possible mechanism of inhibition of osteoclastogenesis by BaP. These results add to the growing evidence that exposure to PAHs affects bone remodeling not only by inhibiting osteoblast differentiation and function [46], but also by directly inhibiting osteoclastogenesis [15,47]. However, from a bone remodeling standpoint, exposure of bone cells to environmental pollutants has much wider implications. Beside the direct inhibition of both osteoblast and osteoclast differentiation processes, BaP induces macrophages and osteoclasts to express CYP1B1. CYP1B1, besides converting BaP to a more toxic metabolite, is an estrogen-metabolizing enzyme [48,49]. Exposure to PAHs or cigarette smoke is known to increase CYP1B1 expression in other tissues [50]; a similar increase of CYP1B1 expression could occur in bone as well. As estrogen is known to play a critical role in bone remodeling [51], a significant decrease in estrogen levels in bone would lead to decreased bone deposition rates, leading to impaired bone remodeling. This could be one of the possible explanations

why cigarette smoking is a risk factor for bone loss in periodontal disease, increased bone fracture rates, and impaired bone healing after surgery [6,7].

## Acknowledgements

We would like to thank Dr. Allan Okey for helpful discussions and for critical reading of the manuscript.

This work was supported by operating grants from the Canadian Institute of Health Research (MOP79322), an equipment grant from the Canada Foundation for Innovation/Ontario Innovation Trust (#7433) and a salary support to IV from CIHR Strategic Training Program in Cell Signaling in Mucosal Inflammation & Pain (STP-53877).

## REFERENCES

- [1] Blanco GA, Cooper EL. Immune systems, geographic information systems (GIS), environment and health impacts. *J Toxicol Environ Health B Crit Rev* 2004;7:465–80.
- [2] Pitts Jr JN, Van Cauwenberghe KA, Grosjean D, Schmid JP, Fitz DR, Belser WL, et al. Atmospheric reactions of polycyclic aromatic hydrocarbons: facile formation of mutagenic nitro derivatives. *Science* 1978;202:515–9.
- [3] Hankinson O. Role of coactivators in transcriptional activation by the aryl hydrocarbon receptor. *Arch Biochem Biophys* 2005;433:379–86.
- [4] Mimura J, Fujii-Kuriyama Y. Functional role of AhR in the expression of toxic effects by TCDD. *Biochim Biophys Acta* 2003;1619:263–8.
- [5] Denison M, Pandini A, Nagy S, Baldwin E, Bonati L. Ligand binding and activation of the Ah receptor. *Chem Biol Interact* 2002;141:3–24.
- [6] Haverstock B, Mandracchia V. Cigarette smoking and bone healing: implications in foot and ankle surgery. *J Foot Ankle Surg* 1998;37:69–74.
- [7] Olofsson H, Byberg L, Mohsen R, Melhus H, Lithell H, Michaelsson K. Smoking and the risk of fracture in older men. *J Bone Miner Res* 2005;20:1208–15.
- [8] Tian Y, Rabson A, Gallo M. Ah receptor and NF- $\kappa$ B interactions: mechanisms and physiological implications. *Chem Biol Interact* 2002;141:97–115.
- [9] Bock KW, Kohle C. Ah receptor: dioxin-mediated toxic responses as hints to deregulated physiologic functions. *Biochem Pharmacol* 2006;72:393–404.
- [10] Boyle W, Simonet W, Lacey D. Osteoclast differentiation and activation. *Nature* 2003;423:337–42.
- [11] Hsu H, Lacey DL, Dunstan CR, Solovyev I, Colombero A, Timms E, et al. Tumor necrosis factor receptor family member RANK mediates osteoclast differentiation and activation induced by osteoprotegerin ligand. *Proc Natl Acad Sci U S A* 1999;96:3540–5.
- [12] Hayden MS, Ghosh S. Signaling to NF- $\kappa$ B. *Genes Dev* 2004;18:2195–224.
- [13] Martin L, Byrd S. Rapid communication: effects of tobacco processing on the quantity of benzo[a]pyrene in mainstream smoke. *J Toxicol Environ Health* 2003;66:1283–6.
- [14] Besaratinia A, Kleinjans JC, Van Schooten FJ. Biomonitoring of tobacco smoke carcinogenicity by dosimetry of DNA adducts and genotyping and phenotyping of biotransformational enzymes: a review on polycyclic aromatic hydrocarbons. *Biomarkers* 2002;7:209–29.

- [15] Voronov I, Heersche JN, Casper RF, Tenenbaum HC, Manolson MF. Inhibition of osteoclast differentiation by polycyclic aryl hydrocarbons is dependent on cell density and RANKL concentration. *Biochem Pharmacol* 2005;70:300–7.
- [16] Nelson DE, Ihekweaba AE, Elliott M, Johnson JR, Gibney CA, Foreman BE, et al. Oscillations in NF-kappaB signaling control the dynamics of gene expression. *Science* 2004;306:704–8.
- [17] Hoffmann A, Levchenko A, Scott ML, Baltimore D. The IkappaB-NF-kappaB signaling module: temporal control and selective gene activation. *Science* 2002;298:1241–5.
- [18] Zou W, Amcheslavsky A, Takeshita S, Drissi H, Bar-Shavit Z. TNF-alpha expression is transcriptionally regulated by RANK ligand. *J Cell Physiol* 2005;202:371–8.
- [19] Beg AA, Sha WC, Bronson RT, Baltimore D. Constitutive NF-kappa B activation, enhanced granulopoiesis, and neonatal lethality in I kappa B alpha-deficient mice. *Genes Dev* 1995;9:2736–46.
- [20] Pahl HL, Krauss B, Schulze-Osthoff K, Decker T, Traenckner EB, Vogt M, et al. The immunosuppressive fungal metabolite gliotoxin specifically inhibits transcription factor NF-kappaB. *J Exp Med* 1996;183:1829–40.
- [21] Ozaki K, Takeda H, Iwahashi H, Kitano S, Hanazawa S. NF-kappaB inhibitors stimulate apoptosis of rabbit mature osteoclasts and inhibit bone resorption by these cells. *FEBS Lett* 1997;410:297–300.
- [22] Herfarth H, Brand K, Rath HC, Rogler G, Scholmerich J, Falk W. Nuclear factor-kappa B activity and intestinal inflammation in dextran sulphate sodium (DSS)-induced colitis in mice is suppressed by gliotoxin. *Clin Exp Immunol* 2000;120:59–65.
- [23] Kishore N, Sommers C, Mathialagan S, Guzova J, Yao M, Hauser S, et al. A selective IKK-2 inhibitor blocks NF-kappa B-dependent gene expression in interleukin-1 beta-stimulated synovial fibroblasts. *J Biol Chem* 2003;278:32861–7.
- [24] Hogan PG, Chen L, Nardone J, Rao A. Transcriptional regulation by calcium, calcineurin, and NFAT. *Genes Dev* 2003;17:2205–32.
- [25] Duyao MP, Buckler AJ, Sonenshein GE. Interaction of an NF-kappa B-like factor with a site upstream of the c-myc promoter. *Proc Natl Acad Sci U S A* 1990;87:4727–31.
- [26] Battaglini R, Kim D, Fu J, Vaage B, Fu X, Stashenko P. c-myc is required for osteoclast differentiation. *J Bone Miner Res* 2002;17:763–73.
- [27] Tian Y, Ke S, Denison MS, Rabson AB, Gallo MA. Ah receptor and NF-kappaB interactions, a potential mechanism for dioxin toxicity. *J Biol Chem* 1999;274:510–5.
- [28] Ruby CE, Leid M, Kerkvliet NI. 2,3,7,8-Tetrachlorodibenzo-p-dioxin suppresses tumor necrosis factor-alpha and anti-CD40-induced activation of NF-kappaB/Rel in dendritic cells: p50 homodimer activation is not affected. *Mol Pharmacol* 2002;62:722–8.
- [29] Takatsuna H, Asagiri M, Kubota T, Oka K, Osada T, Sugiyama C, et al. Inhibition of RANKL-induced osteoclastogenesis by (-)-DHMEQ, a novel NF-kappaB inhibitor, through downregulation of NFATc1. *J Bone Miner Res* 2005;20:653–62.
- [30] Puga A, Barnes SJ, Chang C, Zhu H, Nephew KP, Khan SA, et al. Activation of transcription factors activator protein-1 and nuclear factor-kappaB by 2,3,7,8-tetrachlorodibenzo-p-dioxin. *Biochem Pharmacol* 2000;59:997–1005.
- [31] Banerjee R, Caruccio L, Zhang YJ, McKercher S, Santella RM. Effects of carcinogen-induced transcription factors on the activation of hepatitis B virus expression in human hepatoblastoma HepG2 cells and its implication on hepatocellular carcinomas. *Hepatology* 2000;32:367–74.
- [32] Ding J, Wu K, Zhang D, Luo W, Li J, Ouyang W, et al. Activation of both nuclear factor of activated T cells and inhibitor of nuclear factor-kappaB kinase beta-subunit/nuclear factor-kappaB is critical for cyclooxygenase-2 induction by benzo[a]pyrene in human bronchial epithelial cells. *Cancer Sci* 2007;98:1323–9.
- [33] Camacho IA, Singh N, Hegde VL, Nagarkatti M, Nagarkatti PS. Treatment of mice with 2,3,7,8-tetrachlorodibenzo-p-dioxin leads to aryl hydrocarbon receptor-dependent nuclear translocation of NF-kappaB and expression of Fas ligand in thymic stromal cells and consequent apoptosis in T cells. *J Immunol* 2005;175:90–103.
- [34] Warren GW, Poloyac SM, Gary DS, Mattson MP, Blouin RA. Hepatic cytochrome P-450 expression in tumor necrosis factor-alpha receptor (p55/p75) knockout mice after endotoxin administration. *J Pharmacol Exp Ther* 1999;288:945–50.
- [35] Ke S, Rabson AB, Germino JF, Gallo MA, Tian Y. Mechanism of suppression of cytochrome P-450 1A1 expression by tumor necrosis factor-alpha and lipopolysaccharide. *J Biol Chem* 2001;276:39638–44.
- [36] Bleau AM, Maurel P, Pichette V, Leblond F, du Souich P. Interleukin-1beta, interleukin-6, tumour necrosis factor-alpha and interferon-gamma released by a viral infection and an aseptic inflammation reduce CYP1A1 1A2 and 3A6 expression in rabbit hepatocytes. *Eur J Pharmacol* 2003;473:197–206.
- [37] Morgan ET. Regulation of cytochrome p450 by inflammatory mediators: why and how? *Drug Metab Dispos* 2001;29:207–12.
- [38] Wada T, Nakashima T, Hiroshi N, Penninger JM. RANKL-RANK signaling in osteoclastogenesis and bone disease. *Trends Mol Med* 2006;12:17–25.
- [39] Tanaka S, Nakamura K, Takahashi N, Suda T. Role of RANKL in physiological and pathological bone resorption and therapeutics targeting the RANKL-RANK signaling system. *Immunol Rev* 2005;208:30–49.
- [40] Adhikari A, Xu M, Chen ZJ. Ubiquitin-mediated activation of TAK1 and IKK. *Oncogene* 2007;26:3214–26.
- [41] Deng L, Wang C, Spencer E, Yang L, Braun A, You J, et al. Activation of the IkappaB kinase complex by TRAF6 requires a dimeric ubiquitin-conjugating enzyme complex and a unique polyubiquitin chain. *Cell* 2000;103:351–61.
- [42] Ohtake F, Baba A, Takada I, Okada M, Iwasaki K, Miki H, et al. Dioxin receptor is a ligand-dependent E3 ubiquitin ligase. *Nature* 2007;446:562–6.
- [43] Wu P, Wang P. Per-Arnt-Sim domain-dependent association of cAMP-phosphodiesterase 8A1 with IkappaB proteins. *Proc Natl Acad Sci U S A* 2004;101:17634–9.
- [44] Zhang L, Savas U, Alexander DL, Jefcoate CR. Characterization of the mouse Cyp1B1 gene. Identification of an enhancer region that directs aryl hydrocarbon receptor-mediated constitutive and induced expression. *J Biol Chem* 1998;273:5174–83.
- [45] Zheng W, Jefcoate CR. Steroidogenic factor-1 interacts with cAMP response element-binding protein to mediate cAMP stimulation of CYP1B1 via a far upstream enhancer. *Mol Pharmacol* 2005;67:499–512.
- [46] Singh S, Casper R, Fritz P, Sukhu B, Ganess B, Girard BJ, et al. Inhibition of dioxin effects on bone formation in vitro by a newly described aryl hydrocarbon receptor antagonist, resveratrol. *J Endocrinol* 2000;167:183–95.
- [47] Naruse M, Otsuka E, Naruse M, Ishihara Y, Miyagawa-Tomita S, Hagiwara H. Inhibition of osteoclast formation by 3-methylcholanthrene, a ligand for arylhydrocarbon receptor: suppression of osteoclast differentiation factor in osteogenic cells. *Biochem Pharmacol* 2004;67:119–27.

- 
- [48] Bruno RD, Njar VC. Targeting cytochrome P450 enzymes: a new approach in anti-cancer drug development. *Bioorg Med Chem* 2007;15:5047–60.
- [49] Tsuchiya Y, Nakajima M, Yokoi T. Cytochrome P450-mediated metabolism of estrogens and its regulation in human. *Cancer Lett* 2005;227:115–24.
- [50] Kim JH, Sherman ME, Curriero FC, Guengerich FP, Strickland PT, Sutter TR. Expression of cytochromes P450 1A1 and 1B1 in human lung from smokers, non-smokers, and ex-smokers. *Toxicol Appl Pharmacol* 2004;199:210–9.
- [51] Pacifici R. Estrogen deficiency T cells and bone loss. *Cell Immunol* 2007.